Ionomeric Blends of Poly(ethyl acrylate-*co*-4-vinylpyridine) with Zinc-Neutralized Sulfonated Poly(ethylene terephthalate). 3. Effects of Functionalization Level

C.-W. Alice Ng and William J. MacKnight*

Department of Polymer Science and Engineering, University of Massachusetts, Amherst, Massachusetts 01003

Received July 10, 1995; Revised Manuscript Received November 20, 1995[⊗]

ABSTRACT: This paper constitutes the third part in a series of studies[1,2] on the ionomeric blend system of poly(ethyl acrylate-*co*-4-vinylpyridine) and zinc-neutralized sulfonated poly(ethylene terephthalate). The focus of this work is to examine the compatibility behavior of the system in relation to the functionalization level of the polymer constituents. Particular effort is made to address the competition between the specific interactions that could lead to compatibilization and the crystallization of the semicrystalline component that could lead to phase separation. Results show that compatibilization but not miscibilization was observed with functionalization levels as high as 10 mol %. FTIR studies indicate that the extent of the specific intermolecular interactions between the functionalized polymers increases with the functionalization level. In accordance, the degree of mixing as probed by both differential scanning calorimetry (DSC) and dynamic mechanical thermal analysis (DMTA) also increases as the extent of the specific interactions increases. Crystallization of the PET-SO_3Zn component was shown to induce some phase separation; however, the system remained compatibilized by virtue of the presence of the specific interactions. As a result of the enhanced mixing with an increase in the sulfonation level, the crystallization behavior of the PET-SO_3Zn phase experienced increased perturbation. The mechanical properties of the functionalized blends were shown to exhibit dramatic improvement over that of the unmodified blend, probably as a consequence of interfacial adhesion among the different phases within the blend matrix.

Introduction

Multiphase polymer blends have been of great importance in the development of new synthetic materials. However, the development of new useful blends is severely limited by the complete incompatibility of many polymer pairs of interest. The general challenge of polymer blending is to overcome the low entropy of mixing and unfavorable enthalpy of mixing of most high molecular weight polymers. For many blend systems, high interfacial tension and weak interfacial adhesion lead to ill-defined morphologies with coarsely phase-separated structures and inferior ultimate mechanical properties. One of the basic strategies is to improve the adhesion across phase boundaries in order to control morphology. One approach is to introduce a small amount of ionic moieties into the chains of either or both of the constituent polymers in the blend in order to create specific sites for intermolecular interactions between the otherwise immiscible polymers.[3,4]

Ionomeric blend systems containing predominantly noncrystalline components have been a subject of continuous interest for more than a decade. In recent years, semicrystalline/amorphous blends have received increasing attention in the ionomer field. The systems that have been explored include nylon 4 with lithium-neutralized sulfonated polystyrene,[5] nylon 6 with sulfonated polystyrene[6,7] and poly(ethyl acrylate-*co*-4-vinylpyridine) with zinc-neutralized sulfonated PET.[1,2] The presence of the semicrystalline component adds to the difficulty in assessing the compatibility of the blends. Besides, the compatibilization could potentially be decreased as a result of the crystallization. Hence, it is one of our major emphases in this series of work to understand the influence of the crystalline phase behavior on the overall compatibilization of a semicrystalline/amorphous blend.

This report comprises the third part of a series of studies on the semicrystalline/amorphous ionomeric blend of poly(ethyl acrylate-*co*-4-vinylpyridine) with zinc-neutralized sulfonated poly(ethylene terephthalate). The first two parts of the work have focused on the effects of the stoichiometry of the specific interacting groups upon the natures of both the amorphous and the crystalline phases.[1,2] In this study, the emphasis is on the effects of the functionalization level of the constituent polymers upon the overall compatibility behavior of the system. As mentioned before, particular efforts are made to examine the competing phenomena between the specific intermolecular interactions that could lead to compatibilization and the crystallization of the semicrystalline component that could lead to phase separation. On the other hand, the influence of the compatibility on the crystallization behavior of the sulfonated poly(ethylene terephthalate) component is also investigated by comparing the behavior of the semicrystalline homopolymers with the blend. The effect of the compatibilization introduced as a result of the specific interactions on the large deformation mechanical properties will be assessed by comparing the functionalized blends to their unmodified counterparts.

The ion-containing component of the present blend system is a zinc-neutralized sulfonated poly(ethylene terephthalate). This material has been known for a long time and is usually in the form of the sodium salt with a sulfonation level in the range of 1−2 mol %. It is used for improving the dyeability of the polyester for various applications such as textile fibers.[8] However, the sulfonated poly(ethylene terephthalate) remains to be explored as only a few studies[9−14] have been undertaken to understand this polymer as an ionomer at various levels of sulfonation neutralized with different countercations. The use of different counterions will likely

[⊗] Abstract published in *Advance ACS Abstracts,* February 1, 1996.

0024-9297/96/2229-2412$12.00/0

Table 1. Nomenclature and Characteristics of Constituent Polymers

polymer	designation	mol % VP or SO_3Zn	M_n	M_w/M_n
poly(ethyl acrylate)	PEA	0	230 000	3.87
poly(ethy acrylate-*co*-4-vinylpyridine)	2EAVP	2.4	230 000	3.17
	5EAVP	5.2	201 000	2.02
	10EAVP	10.6	161 000	1.96
poly(ethylene terephthalate)	PET	0	IV[a] = 0.62	
zinc-neutralized sulfonated PET	2PET-SO_3Zn	2	IV = 0.44	
	4PET-SO_3Zn	4	IV = 0.45	
	10PET-SO_3Zn	10	IV = 0.35	

[a] IV is the inherent viscosity measured in dL/g for the sulfonated PET in sodium salt form.

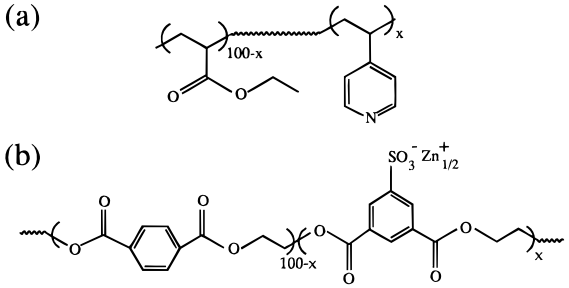

Figure 1. Chemical structures of (a) EAVP and (b) PET-SO_3-Zn where *x* denotes the mole percent of functionalization.

Table 2. Nomenclature and Compositions of Polymer Blends

polymer	designation	wt % PEA or EAVP	wt % PET or PET-SO_3Zn
PEA/PET-50/50	0B	50	50
2EAVP/2PET-SO_3Zn-50/50	2B	50	50
5EAVP/4PET-SO_3Zn-45/55	5B	45	55
10EAVP/10PET-SO_3Zn-50/50	10B	50	50

influence the behavior of the ionomer as well as its interaction with other functionalized polymer chains. Therefore, in a later paper as the fourth part of this series of studies, the effects of counterion on the behavior of the ionomer and its compatibility with poly(ethyl acrylate-*co*-4-vinylpyridine) will be discussed.[15]

Experimental Section

Materials Used. Poly(ethyl acrylate) (PEA) and poly(ethyl acrylate-*co*-4-vinylpyridine) (EAVP) with different vinylpyridine (VP) contents (2, 5, and 10 mol % VP) were prepared by free-radical polymerization and were characterized previously.[16] Poly(ethylene terephthalate) (PET) and sodium-neutralized sulfonated PET (PET-SO_3Na) with 2 mol % sulfonation were generously supplied by E. I. du Pont de Nemours. The 4 and 10 mol % PET-SO_3Na were kindly supplied by AKZO Corporate Research, Arnhem, Holland. The sulfonation levels of the various PET-SO_3Na were confirmed by elemental analysis.[17] The PET-SO_3Na's were then subjected to an ion-exchange procedure developed in our laboratory[1] to replace the sodium with zinc ion to yield PET-SO_3Zn. The chemical structures of the polymers are schematically shown in Figure 1. The nomenclature and characteristics of the constituent polymers are summarized in Table 1.

Blend Preparation. Blends containing stoichiometric amounts of vinylpyridine groups and sulfonate groups were prepared by solution blending. An unmodified blend containing no interacting groups in both polymers was also prepared for comparison purposes. In addition, the blend compositions were kept almost the same for all samples. The composition and nomenclature of the blends prepared are listed in Table 2.

Individual constituent polymers were predried at 60 °C under vacuum for 1 day prior to use. The constituent polymers were separately dissolved in 1,1,1,3,3,3-hexafluoro-2-propanol (HFIP) to yield a 5% (w/v) polymer solution. The PEA or EAVP solution was added to the PET-SO_3Zn solution under vigorous stirring. Due to the gelation in blends of high functionalization level, all blend solutions were heated to 70 °C for 5 h in a nitrogen atmosphere to ensure thorough mixing. The polymer solution was then cast onto a Teflon dish under a slow stream of nitrogen. After most of the solvent was removed at ambient conditions, the polymer film was allowed to dry at 60 °C for 3 days under vacuum.

Molecular Weight Determination. The molecular weights of PEA and the various EAVP's were determined by GPC as reported.[16] For PET and the various PET-SO_3Na's, inherent viscosity measurements were performed using a Cannon-Ubbelohde viscometer at 30 °C in trifluoroacetic acid. The polymer concentration was about 0.5 g/dL. The results are summarized in Table 1.

FTIR Study. Infrared spectra were obtained on an IBM IR44 FTIR spectrometer. A total of 128 scans at a resolution of 1 cm^{-1} were signal averaged. Samples were dissolved in HFIP solution and were cast into thin films on a flat Teflon sheet under a slow stream of nitrogen. The concentrations of the solutions used ranged from 2 to 6% (w/v). The thin films were further dried at 60 °C for 3 days under vacuum.

DSC Measurements. A Perkin-Elmer DSC-7 was used to obtain DSC thermograms and was calibrated with indium and water. Experiments were run with samples ranging from 5 to 10 mg under a dry nitrogen purge to prevent moisture and oxidative degradation. To obtain the thermal behavior of the as-cast films, the samples were equilibrated at −50 °C and heated to the molten state (270 °C for 0B and 2B; 250 °C for 5B and 10B) at 10 °C/min. Quenched samples of both the blends and the constituent polymers were obtained by heating in the molten state for 5 min and quickly quenching to −50 °C. The thermal behavior of the quenched samples was probed by heating from −50 °C to the molten state at a rate of 10 °C/min. Annealed samples were obtained by annealing the quenched samples at 150 °C for 15 min and the thermal behavior was examined as described above. The glass transition temperatures (T_g) were taken as the midpoints of the change in heat capacity. The melting temperatures (T_m) and the crystallization temperatures (T_c) were taken as the peaks of the transitions. The heat of fusion (ΔH_m) and heat of crystallization (ΔH_c) were measured by calculating the area under the appropriate endothermic or exothermic peaks and were normalized per gram of the semicrystalline component in the blends. The percent crystallinity of the crystallized samples was estimated by assuming an enthalpy of melting of 113 J/g for 100% crystalline PET.[18]

DMTA Measurements. Dynamic mechanical properties were measured using a Polymer Laboratories PL-DMTA instrument at a frequency of 1 Hz. Quenched samples were prepared by compression molding under low pressure and a nitrogen atmosphere in the molten state for 1 min to erase the thermal history and were cooled quickly between two cold metal plates. Solution-cast blend samples were cut into appropriate sizes and examined as-cast. The PEA and EAVP samples were compression molded between sheets of aluminum foil at 50 °C. Due to the brittleness of the PET-SO_3Zn polymers, films could not be prepared. All specimen sizes were approximately 25 mm × 13 mm × 0.5 mm. Experiments were performed in a single-cantilever mode using a 5.2-mm free length and were scanned from −100 to +200 °C at a rate of 3 °C/min. The T_g's were taken as the peaks in the tan δ plots. The modulus data were treated with the PL-DMTA end correction software to correct for sample clamping efficiency.

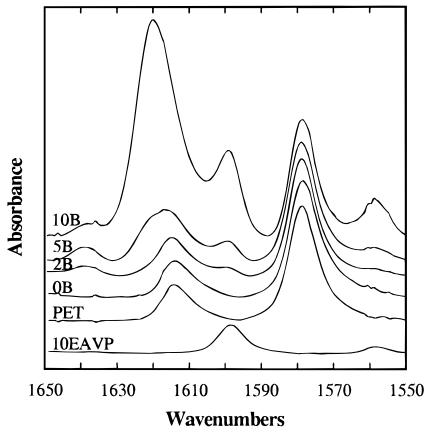

Figure 2. FTIR spectra for 10EAVP, PET, and blends of 0B, 2B, 5B, and 10B.

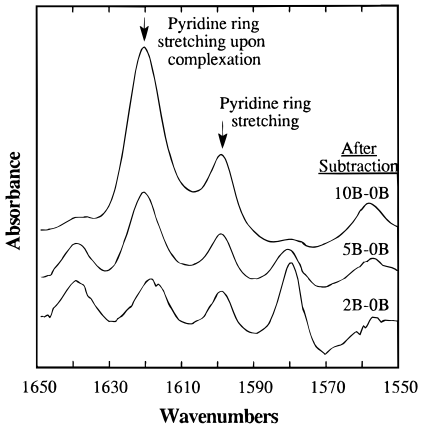

Figure 3. FTIR spectra for 2B, 5B, and 10B blends after subtraction; the subtraction was performed based on the peak at 1580 cm^{-1}.

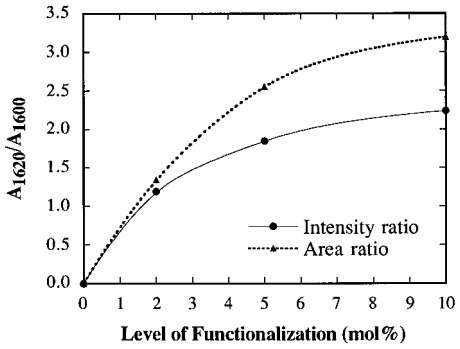

Figure 4. Extent of specific intermolecular interactions (A_{1620}/A_{1600}) versus functionalization level of blends of 0B, 2B, 5B, and 10B.

Tensile Measurements. Uniaxial stress−strain data were obtained with an Instron Model 4202 testing instrument equipped with a series IX automatic materials testing system for automatic data acquisition. Solution-cast samples were used and cut into thin strips of approximately 6 mm × 0.5 mm × 80 mm. Experiments were run with an initial gauge length of 40 mm at a constant crosshead speed of 4 mm/min at room temperature. Three to five samples were examined for each material and the results averaged.

SEM Measurements. A JEOL JSM-35CF scanning electron microscope operating at 20 kV was used to examine fracture surfaces. Compression-molded samples were prepared and were freeze fractured at liquid nitrogen temperature. The samples were coated with a thin layer of gold for examination under the microscope.

Results and Discussion

Nature of Specific Interactions. Understanding the nature and extent of specific interactions between functional groups of two different types of polymer chains is fundamental to the elucidation of the structure−property relationship of ionomeric blends. In this section, we will be examining the effects of functionalization level upon the nature and extent of specific interactions between the otherwise immiscible polymer pair.

Figure 2 shows the IR spectra for the constituent polymers, 10EAVP and PET, and the blends. Based on the peak assignments reported in a previous publication,[1] the peak at 1600 cm^{-1} is assigned as the free pyridine ring stretching and the peak at 1620 cm^{-1} as the pyridine ring stretching upon complexation between the zinc metal and the pyridine ring. However, this study shows that the peak position of the complexed pyridine ring stretching varies with the functionalization level. A closer look at the spectra of both the unmodified blend 0B and pure PET reveals that the observed peak shift might be due to an overlap with a small peak at 1615 cm^{-1} contributed by the parent PET component. The peak shift becomes large when the peak intensity of the complexed ring stretching is small compared to the peak at 1615 cm^{-1}. Hence, a subtraction to remove the peak at 1615 cm^{-1} was necessary to clearly reveal the spectral changes due to the specific interactions. Figure 3 shows the subtracted spectra for the 2B, 5B, and 10B blends. The peak assignments of the complexed ring stretching are in good agreement with our previous findings. Moreover, the peak widths of the complexed ring stretching are similar among the modified blends, which suggests that the nature of the complexation remains the same irrespective of the functionalization level. The relative extent of the interaction, represented by the ratio of either the peak intensity or peak area of A_{1620} to A_{1600}, is found to increase with the level of functionalization as illustrated in Figure 4. The similar trend exhibited by both ratios further confirms the invariant nature of the complexation among the modified blends. Despite the fact that all blends contain stoichiometric amounts of both interacting groups, the specific complexation remains incomplete at all functionalization levels. This might be due to the fact that the probability for the interacting groups to find each other for complexation is lowered by the steric constraints imposed on these groups by the chain itself and the isolation of the interaction sites. Nevertheless, the probability for complexation can be enhanced by increasing the functionalization level of both polymers as observed.

Compatibility Behavior. The compatibility of the ionomeric blends is examined by DSC and DMTA. It is well known that the phase behavior of a polymer blend is dependent upon its sample history, in particular those containing a semicrystalline component. Hence, the phase behavior of the blends in both amorphous/amorphous and amorphous/semicrystalline states is compared and contrasted. In particular, efforts are made to assess the influence of the crystallization on the overall compatibility of the system.

DSC Study. Table 3 summarizes the glass transition behavior of both series of homopolymers. The T_g of the poly(ethyl acrylate) series is shown to increase with increasing VP content. This is because the VP monomer imposes a stiffening effect on the polymer backbone. On the other hand, the T_g of the PET series is found to

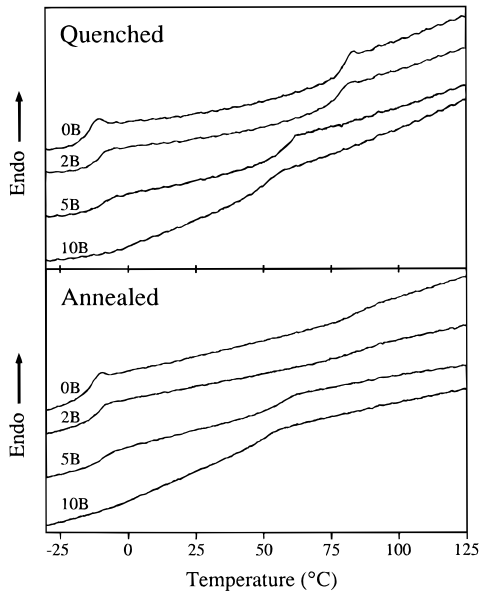

Figure 5. DSC thermograms showing the glass transition behavior of the quenched and annealed blends of 0B, 2B, 5B, and 10B.

Table 3. DSC Results: T_g's for the Constituent Polymers and the Blends in the Quenched State

polymer	T_{g1} (°C)	ΔT_{g1} (°C)	T_{g2} (°C)	ΔT_{g2} (°C)
0B	−15	4	79	7
2B	−11	7	77	9
5B	−10	13	57	14
10B	16	16	49	17
PEA	−16	4		
2EAVP	−14	5		
5EAVP	−12	5		
10EAVP	−6	6		
PET			78	5
2PET-SO_{3Zn}			78	8
4PET-SO_{3Zn}			64	8
10PET-SO_{3Zn}			61	14

decrease with increasing sulfonation level. Such behavior is directly opposite to that observed for other sulfonate ionomers such as sulfonated polystyrene which shows an increase in T_g with sulfonation as a result of the ionic interactions that limit the chain mobility. In the case of sulfonated PET, the decrease in molecular weight with increasing sulfonation level may be partly responsible. Further studies are needed to clarify this point.

Figure 5 shows the DSC thermograms of both the quenched and annealed blends. It is shown that all the quenched samples exhibit two T_g's which become broadened and less distinct at increasing levels of functionalization. Table 3 summarizes the T_g measurements of the quenched blends in comparison to those of their constituent polymers. Except for the unmodified 0B blend, where there are virtually no changes in both the T_g and ΔT_g compared with their homopolymers, all the modified blends show an increase in T_{g1} of the EAVP phase and a decrease in T_{g2} of the PET-SO_3Zn phase. The ΔT_g's of the blends also increase compared to those of the constituent polymers. In particular, the T_g shifts and their broadening increase with the level of functionalization, which implies that better mixing with increasingly diffuse interfaces is achieved by virtue of the increasing amount of specific interactions in these compatibilized blends, observed in the FTIR study.

Table 4. DSC Results: T_g's for the Constituent Polymers and the Blends in the Annealed State

polymer	T_{g1} (°C)	ΔT_{g1} (°C)	T_{g2} (°C)	ΔT_{g2} (°C)	% crystallinity
0B	−16	8	86	20	30
2B	−13	9	86	27	35
5B	−10	12	55	16	22
10B	35	74			7
PEA	−16	4			
2EAVP	−14	5			
5EAVP	−12	5			
10EAVP	−6	6			
PET			83	23	27
2PET-SO_{3Zn}			82	18	26
4PET-SO_{3Zn}			66	10	4
10PET-SO_{3Zn}			63	15	4

When the PET-SO_3Zn component is allowed to crystallize, the phase composition changes as a function of the degree of crystallinity, which will in turn affect the compatibility behavior of the blends. Table 4 shows the T_g measurements of the annealed blends, PET and PET-SO_3Zn homopolymers.

It is shown that the T_g and ΔT_g of both pure PET and sulfonated PET increase upon annealing of their quenched counterparts. Such an increase in T_g, as reported in our previous communication,[1] is attributed to the stiffening effect on the amorphous phase exerted by the newly formed crystalline domains. In addition, the T_g broadening is shown to be related to the crystallization of the PET-SO_3Zn component in its amorphous phase, which creates a new range of microenvironments for segmental motions, thereby broadening the accompanying glass transition. It is noted in this study that the extent of the increase in T_g and ΔT_g is dependent upon the amount of crystallization taking place. Therefore, under the same annealing conditions, the less functionalized blends which attain a higher degree of crystallinity show a larger increase in both T_g and ΔT_g.

Comparing the quenched and annealed blends, the T_{g2} and ΔT_{g2} of the PET-SO_3Zn phase are found to increase upon annealing. Based on the behavior of the PET-SO_3Zn and PET homopolymers, it is believed that such an increase is associated with the crystallization effect of the PET-SO_3Zn phase, instead of a phase separation phenomenon. When comparing the annealed blends with the annealed PET-SO_3Zn homopolymers, it is found that the T_{g2} of the 2B blend becomes similar to that of its pure constituent polymer, suggesting that some phase separation might have occurred during the annealing process. On the other hand, the 5B annealed blend still shows a lower T_{g2} of the PET-SO_3Zn phase compared to that of its annealed homopolymer, indicating that the blend remains compatibilized. For the 10B blend, it is found that the glass transitions of the quenched blend are collapsed into one broad transition upon annealing, which tends to suggest an enhancement in compatibility. However, based on the findings from the semicrystalline homopolymers, such apparent change is more likely associated with the crystallization of the PET-SO_3Zn component in the vicinity of both the amorphous EAVP and PET-SO_3Zn phase, resulting in the broadening of the already diffuse T_g.

It is apparent that the change in phase behavior of the PET-SO_3Zn component in the annealed samples, while dominated by the crystallization effects, does not yield conclusive evidence on how the overall compatibility behavior of the crystallized blends is affected.

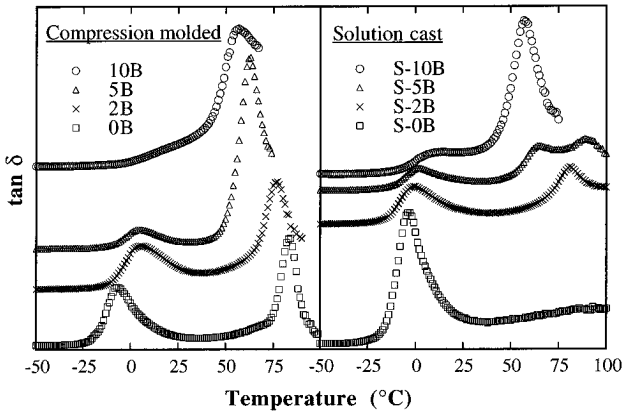

Figure 6. Temperature dependence of tan δ for the compression-molded and solution-cast blends of 0B, 2B, 5B, and 10B recorded at 1 Hz at a scan rate of 3 °C/min.

Table 5. DMTA Results: tan δ for the Constituent Polymers and the Blends in the Quenched and Solution-Cast States

	quenched				solution-cast				
	tan δ_{peak} (°C)		peak width at half-height (°C)		tan δ_{peak} (°C)		peak width at half-height (°C)		% crystallinity[a]
polymer	T_{g1}	T_{g2}	ΔT_{g1}	ΔT_{g2}	T_{g1}	T_{g2}	ΔT_{g1}	ΔT_{g2}	
0B	−7	84	19	11	−4	88	17	broad	35
2B	6	77	28	16	−1	81	25	25	48
5B	5	63	23	15	2	65	26	37	32
10B	15	58	broad	broad	11	57	30	19	5
PEA	−1		11						
2EAVP	−1		11						
5EAVP	1		10						
10EAVP	6		12						
PET		82		10					

[a] % crystallinity obtained from DSC.

However, the noncrystallizable EAVP phase might offer better insight. It is found that the T_{g1}'s of the EAVP phase in the annealed blends show no apparent shift as a consequence of the annealing, which could imply that no significant phase separation is detected due to the crystallization of the PET-SO_3Zn component. In addition, the ΔT_g's of the EAVP phase increase or remain the same, which further suggests that the blends remain compatiblized.

DMTA Study. Due to the inherent limit in sensitivity of the DSC technique, the subtle but sometimes important changes in mixing behavior might not be probed with sufficient resolution by DSC, in particular in the case of diffuse glass transition behavior. Hence, the compatibility behavior is further examined by DMTA, which offers a more sensitive probe into the mixing behavior of polymer blends.[19] Figure 6 shows the temperature dependence of tan δ of both the compression-molded and solution-cast blends. The results are summarized in Table 5. It is found that the compression-molded samples exhibit two distinct glass transitions except for the 10B blend, where the low-temperature peak at about 6 °C appears as a small shoulder to the high-temperature peak. The findings are in general similar to those obtained by DSC. Nevertheless, the small but distinct degree of compatibility of the 2B blend becomes more distinguishable from the incompatible 0B blend by DMTA. Unlike the macrophase-separated 0B blend with the two relaxation peaks well separated, the 2B blend exhibits continuous relaxation activity throughout the region between the two major relaxation peaks as shown by the nonzero tan δ value. This suggests that a distinct amount of interfacial material exists between the two polymer bulk phases. The distinct increase in both T_{g1} and ΔT_{g1} of the blend compared to those of the homopolymer further confirms the compatibilization occurring in the 2B blend.

For the solution-cast blends, the glass transitions remain distinct by DMTA unlike those observed in the DSC annealing study. In particular, the solution-cast samples have similar crystallinity content to their annealed counterparts as shown in Tables 4 and 5. In addition, it is clearly shown that the low-temperature peak T_{g1} corresponding to the EAVP phase undergoes a consistent decrease in temperature compared to their compression-molded counterparts. However, this is not observed in the DSC study due to the limited sensitivity of the technique itself. The decrease in T_{g1} is probably associated with the enrichment of the EAVP component in the EAVP phase due to the crystallization and thus depletion of the amorphous PET-SO_3Zn component in that phase during the solution-casting. It also implies that some phase separation might have occurred as a result of the crystallization. Nevertheless, the modified blends remain compatibilized as shown by the broadness of the glass transition of the EAVP phase in comparison to those of the pure EAVP homopolymers. For the PET-SO_3Zn phase, there is a similar increase in both T_{g2} and ΔT_{g2} for the solution-cast samples compared to their compression-molded counterparts as observed before. Such an increase has been associated with the crystallization of the PET-SO_3Zn component as concluded from the DSC study. It is also noted that the high-temperature peak T_{g2} exhibits a significant reduction in intensity in the solution-cast samples as compared to their compression-molded counterparts with the exception of the 10B blend. Such a decrease in the relaxation intensity is attributable to the crystallization of the PET or PET-SO_3Zn bulk phase, thereby reducing the amount of amorphous constituent which would otherwise contribute to the relaxation phenomenon accompanying the glass transition in that phase.

Determination of Interfacial Compositions. As shown by both DSC and DMTA studies, the modified PEA/PET blend system exhibits microphase-separated morphologies. Results also indicate that the degree of compatibilization is enhanced with increasing level of functionalization of both polymers. It is known that the interfacial interactions among the different components in a microphase-separated blend matrix are important in controlling the phase morphologies and hence the ultimate properties of the materials. Therefore, the determination of interfacial compositions as a measure of the interfacial interactions should provide further insight in our understanding of the compatibility behavior in relation to the difference in the level of functionalization.

The weight fraction (W_I) of the blend constituents comprising the interphase of a microphase-separated amorphous polymer blend can be estimated from DSC measurements. According to the equation proposed by MacKnight et al.,[20]

$$W_I = 1 - \frac{\Delta C_{p2}[\Delta C_{p2}^\circ \ln(T_{g2}^\circ/T_{g2}) - \Delta C_{p1}^\circ \ln(T_{g1}^\circ/T_{g2})]}{\Delta C_{p1}^\circ \Delta C_{p2}^\circ \ln(T_{g2}^\circ/T_{g1}^\circ)} - \frac{\Delta C_{p1}[\Delta C_{p2}^\circ \ln(T_{g2}^\circ/T_{g1}) - \Delta C_{p1}^\circ \ln(T_{g1}^\circ/T_{g1})]}{\Delta C_{p1}^\circ \Delta C_{p2}^\circ \ln(T_{g2}^\circ/T_{g1}^\circ)} \quad (1)$$

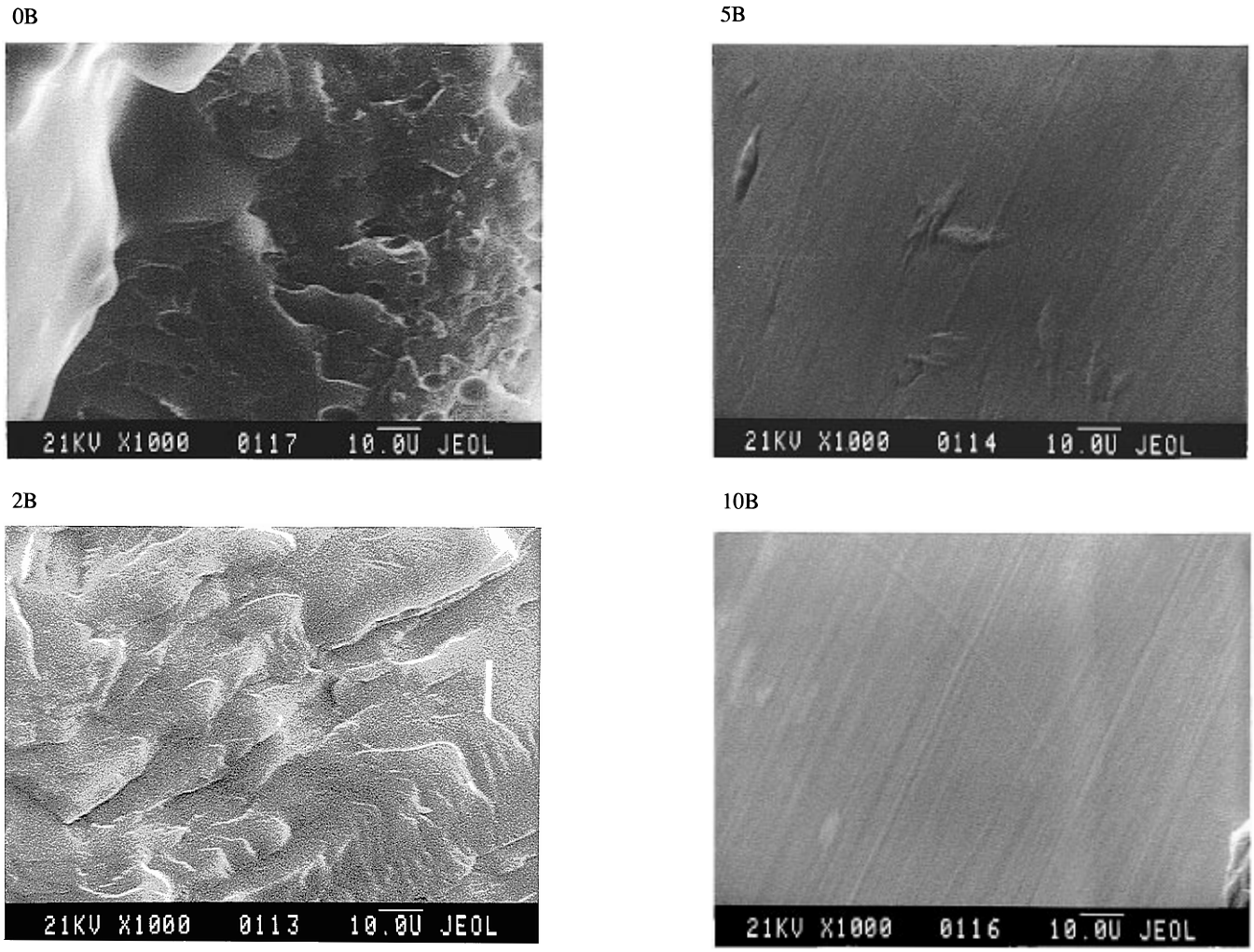

Figure 7. SEM micrographs for freeze-fracture surfaces of compression-molded blends of 0B, 2B, 5B, and 10B.

Table 6. Determination of Interfacial Compositions of the Quenched Blends from DSC Measurements

polymer	W_I
0B	0
2B	0.05
5B	0.21
10B	0.43

where $T_{g1}°$ and $T_{g2}°$ are the T_g's of the constituents before mixing; T_{g1} and T_{g2} are the T_g's of the constituents after mixing; $\Delta C_{p1}°$ and $\Delta C_{p2}°$ are the step increases in heat capacity at the T_g's of the constituents before mixing; and ΔC_{p1} and ΔC_{p2} are the corresponding step increases in heat capacity in the blend.

The results for W_I's of the blends in the amorphous/amorphous state are summarized in Table 6. The unmodified 0B blend shows absolutely no mixing at the interface as expected of a macrophase-separated blend. The modified blends show an increase in the amount of material at the interface as the functionalization level of both polymer components increases. Based on the thermodynamics of blend mixing, the major driving force for enhanced mixing is derived from the presence of the specific intermolecular interactions among the incorporated functional groups. This correlation is supported by the FTIR findings, which show an increase in the extent of specific interactions in response to the increase in the functionalization level. Therefore, it follows that a large extent of the mixing should take place preferably at the interface. On the other hand, the fracture surfaces as depicted in Figure 7 are found to change from rough to smooth with increasing functionalization levels. It is speculated that these morphological changes might be associated with the change in domain sizes of individual phases due to the increase in the amount of mixing at the interface. The domain sizes are forced to reduce in size in order to increase the overall surface area for specific interactions to occur at the interface. However, more detailed morphological work is needed to confirm the proposition.

Crystallization and Melting Behavior. Figure 8 shows the DSC thermograms of the blends, the PET, and the PET-SO_3Zn in their quenched states in the range of 100−270 °C. The transition temperatures and the corresponding enthalpies are listed in Table 7. For the zinc-neutralized sulfonated PET homopolymers, both the melting and crystallization temperatures decrease with increasing level of sulfonation compared to those of pure PET, until the sulfonation content reaches 10 mol %, whereby the crystallization becomes totally suppressed. This can be attributed to (1) the increasing amount of the sulfonated isophthalate monomer units along the polymer chain, which leads to a decrease in chain packing efficiency; and (2) the presence of interactions among the zinc sulfonate ion pairs (or multiplet formation),[12] which further inhibits the crystallization of the PET chains. When pure PET is blended with PEA, the melting behavior remains the same as that of the PET homopolymer as typical of a macrophase-separated blend. For the 2B blend, the thermal behavior is very similar to that of its homopolymer counter-

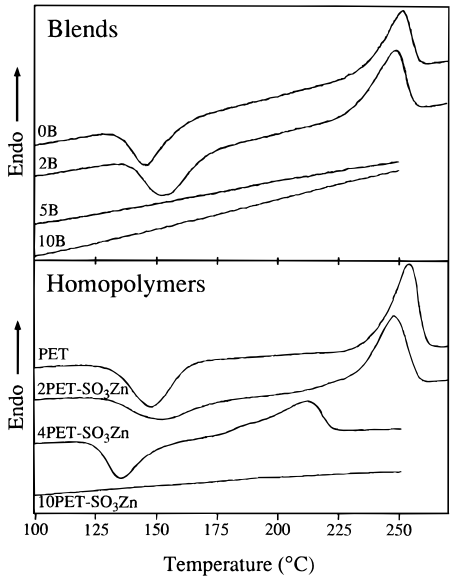

Figure 8. DSC thermograms showing the melting and crystallization behavior of the blends (0B, 2B, 5B, and 10B) and their constituent polymers (PET and PET-SO_3Zn) in the quenched state.

Table 7. DSC Results: Melting and Crystallization Behavior of PET, PET-SO_3Zn, and the Blends in the Quenched State

polymer	T_c (°C)	ΔH_c (J/g)	T_m (°C)	ΔH_m (J/g)
0B	146	−30	251	34
2B	153	−36	249	40
5B				
10B				
PET	148	−31	253	40
2PET-SO_3Zn	152	−27	247	41
4PET-SO_3Zn	136	−25	212	26
10PET-SO_3Zn				

parts except that the crystallization exotherm narrows. The minimal disturbance to the crystallization behavior of the PET-SO_3Zn phase is probably due to the observed low level of mixing of the bulk phases. For the 5B blend, the crystallization of the PET-SO_3Zn phase is completely suppressed unlike that of its homopolymer counterparts, which crystallize under the same experimental conditions. This implies that the crystallization of the PET-SO_3Zn phase is inhibited as a result of the higher level of mixing occurring in the blend matrix. The 10B blend, which has the highest degree of mixing among the blends examined, shows absolutely no crystallization or melting behavior. While the high level of mixing might have an influence, the high sulfonation content is believed to be the major factor leading to the total suppression of the crystallization activity.

When the blends were further annealed or solution cast in HFIP solvent, crystallization occurred in all blends. The resulting melting behaviors are shown in Figure 9. The 2B blend in both the annealed and solution-cast states shows similar melting behavior as the quenched state except for the absence of the crystallization peaks. Unlike the quenched 5B blend, both crystallized samples show a broad melting transition at 195 °C, with the peak temperature increasing slightly for the solution-cast sample. The difference in melting temperature of the crystallized 5B blends may be ascribed to a more perfect crystal formation in the presence of solvent and a longer time of crystallization. For the 10B blend, only a very small melting transition at about 180 °C is observed for both crystallized

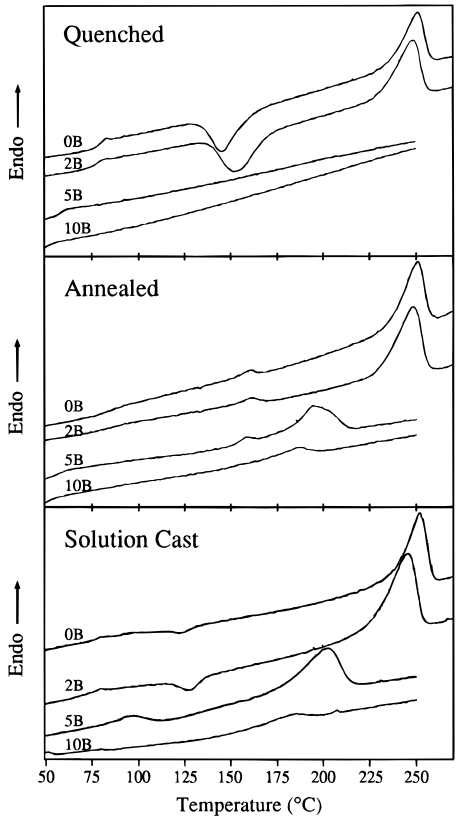

Figure 9. DSC thermograms showing the melting and crystallization behavior of the 0B, 2B, 5B, and 10B blends in the quenched, annealed, and solution-cast states.

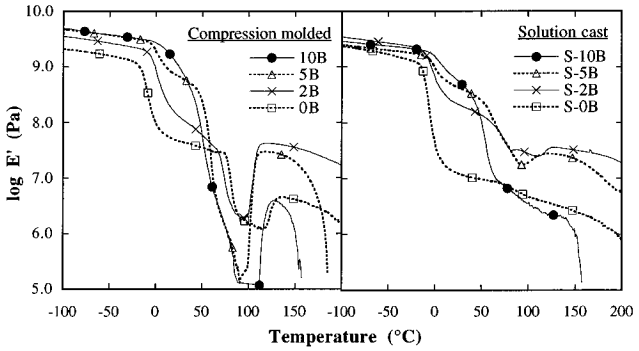

Figure 10. Temperature dependence of the storage modulus (log E') for the compression-molded and solution-cast blends of 0B, 2B, 5B, and 10B recorded at 1 Hz at a scan rate of 3 °C/min.

samples. The disproportionate decrease in both the melting temperatures and the degree of crystallinity at increasing functionalization levels are attributed to the increase in mixing and sulfonation level of the PET chains, thereby affecting both the rates and perfection of the crystal formation among the blends.

Mechanical Properties. Figure 10 shows the temperature dependence of the storage modulus (E') of the compression-molded and solution-cast blends. At 25 °C, log E' is found to increase with the level of functionalization irrespective of the differences in the degree of crystallinity between the two sets of samples. Such increase in the modulus is probably due to the synergistic reinforcement of the glassy phase by the rubbery component by virtue of the increasing interfacial adhesion throughout the blend matrix. However, when the material reaches its rubbery state, the plateau modulus exhibits an optimum at an intermediate functionalization level, instead of a monotonic increase, as illustrated

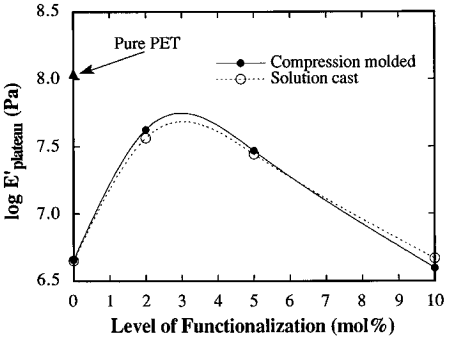

Figure 11. Comparison of the log of the plateau modulus as a function of functionalization level for the compression-molded and solution-cast blends of 0B, 2B, 5B, and 10B.

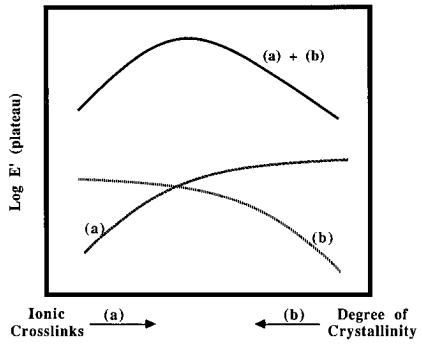

Figure 12. Schematic explanation of Figure 11.

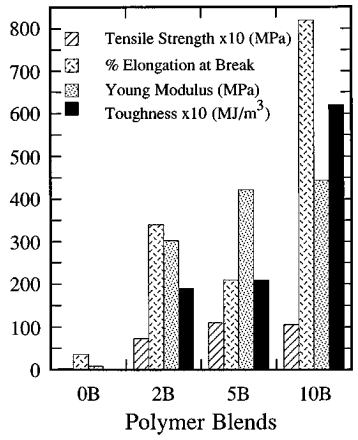

Figure 13. Comparison of the tensile properties of the solution-cast blends of 0B, 2B, 5B, and 10B.

in Figure 11. It is known that the material properties in the rubbery plateau region are governed by factors such as the molecular weight, the amount of cross-linking, and the degree of crystallinity present in the semicrystalline polymers. In this particular blend system, both the cross-linking density (via specific interactions) and the crystalline component exert their own influence in the plateau region as shown in the schematics proposed in Figure 12. The fact is that an increase in the cross-linking density always results in a corresponding decrease in the degree of crystallinity as discussed above. As a consequence, the plateau modulus reflects the combined effects of the opposing factors and thus exhibits a maximum at an intermediate functionalization level.

Figure 13 summarizes the tensile properties of the solution-cast blends at room temperature. It is clear that the modified blends undergo dramatic improvement in the overall tensile properties in comparison to the unmodified, macrophase-separated 0B blend despite the fact that the pure PET-SO_3Zn ionomers are of low molecular weight and exhibit very poor mechanical properties. Continuous enhancement in the properties is observed among the modified blends with increasing levels of functionalization of both polymers. In particular for the 2B blend, a fourfold increase in toughness is obtained with only 2 mol % of functionalization of both polymers, which have been shown to exhibit a minimal amount of mixing. The extremely large elongation (up to 800%) of the 10B blend is indeed an unusual feature in the material properties with this particular blend system. Such a remarkable improvement in properties is a direct result of the favorable interfacial adhesion occurring by virtue of the specific interactions among the functionalized polymers. More importantly, such findings help to illustrate the fundamental fact that specific interactions can be successfully and effectively utilized as a tool to promote the interfacial adhesion between different phases in a polymer matrix, which can ultimately enhance the overall material properties. Furthermore, the unique combination of the rubbery and glassy polymer components whereby the glassy phase is capable of further alignment upon stretching allows further improvement in the tensile performance of the system.

Conclusions

Compatibilization of an otherwise immiscible PEA/PET blend is achieved by virtue of the presence of the specific intermolecular interactions between the functionalized polymer pair as evidenced by the FTIR study. The extent of the specific interactions between the zinc sulfonate groups of the PET chains and the pyridine groups of the PEA chains increases when the functionalization levels of both polymers increase. The degree of compatibilization is found to increase with the functionalization level as shown by the T_g measurements using both DSC and DMTA. Even at the highest level of functionalization, 10 mol %, complete miscibility is not achieved. The degree of the interfacial mixing is further quantified using the phase composition calculation, and the results are in good agreement with the thermal analysis study. Results also indicate that the crystallization of the PET-SO_3Zn component has induced a certain degree of phase separation. However, the system remains compatibilized by virtue of the presence of the specific interactions. On the other hand, the crystallization and melting behavior of the PET-SO_3-Zn phase were suppressed to various extents due to the increase in the level of phase mixing and the sulfonation level of the PET chains. The functionalized PEA/PET blends exhibit remarkable improvement in the ultimate mechanical properties as compared to the unmodified counterparts.

Acknowledgment. The authors gratefully acknowledge the financial supports received from the Materials Research Laboratory at the University of Massachusetts, supported by the National Science Foundation and the Center for University of Massachusetts Industry Research on Polymers (CUMIRP).

References and Notes

(1) Ng, C.-W. A.; Lindway, M. J.; MacKnight, W. J. *Macromolecules* **1994**, *27*, 3027.
(2) Ng, C.-W. A.; MacKnight, W. J. *Macromolecules* **1994**, *27*, 3033.
(3) Ottenbrite, R. M.; Utracki, L. A.; Inoue, S., Eds. *Current Topics in Polymer Science*; Hanser Verlag: Munchen, 1987.

(4) Utracki, L. A.; Weiss, R. A. *Multiphase Polymers: Blends and Ionomers*; Advances in Chemistry 395; American Chemical Society: Washington, DC, 1989.
(5) Ng, C.-W. A.; Bellinger, M. A.; MacKnight, W. J. *Macromolecules* **1994**, *27*, 6942.
(6) Molnar, A.; Eisenberg, A. *Macromolecules* **1992**, *25*, 5774.
(7) Lu, X.; Weiss, R. A. *Macromolecules* **1992**, *25*, 6185.
(8) Ostrowska, J.; Ostrowska-Gumkowska, B.; Rybinska, D.; Szymanski, G. *Acta Polym*. **1985**, *36* (12), 691.
(9) Greener, J.; Gillmor, J. R.; Daly, R. C. *Macromolecules* **1993**, *26*, 6416.
(10) Timm, D. A.; Hsieh, Y.-L. *J. Polym. Sci., B: Polym Phys.* **1993**, *31*, 1873.
(11) Timm, D. A.; Hsieh, Y.-L. *J. Appl. Polym. Sci.* **1994**, *51*, 1291.
(12) Ostrowska-Czubenko, J.; Ostrowska-Gumkowska, B. *Eur. Polym. J.* **1988**, *24* (1), 65.
(13) Ostrowska-Gumkowska, B.; Ostrowska-Czubenko, J. *Eur. Polym. J.* **1988**, *24* (8), 803.
(14) Ostrowska-Gumkowska, B.; Ostrowska-Czubenko, J. *Eur. Polym. J.* **1991**, *27* (7), 681.
(15) Ng, C.-W. A.; MacKnight, W. J. *Macromolecules* **1996**, *29*, 2421.
(16) Douglas, E.; Sakurai, K.; MacKnight, W. J. *Macromolecules* **1991**, *24*, 6776.
(17) The elemental analysis was performed at the Microanalysis Laboratory at the University of Massachusetts, Amherst.
(18) Brandrup, J.; Immergut, E. H. *Polymer Handbook*, 3rd ed.; Wiley: New York, 1989; pp v73.
(19) Stoelting, J.; Karasz, F. E.; MacKnight, W. J. *Polym. Eng. Sci.* **1970**, *10*, 133.
(20) Beckman, E. J.; Karasz, F. E.; Porter, R. S.; Hunsel, J. Van; Koningsveld, R.; MacKnight, W. J. *Macromolecules* **1988**, *21* (4), 1193.

MA950973X